Available online at www.sciencedirect.com
ScienceDirect
Journal of Pharmaceutical and Biomedical Analysis 46 (2008) 920–928
JOURNAL OF PHARMACEUTICAL AND BIOMEDICAL ANALYSIS
www.elsevier.com/locate/jpba

Preparative enantiomeric separation of potent AMP-activated protein kinase activator by HPLC on amylose-based chiral stationary phase Determination of enantiomeric purity and assignment of absolute configuration

Marie-Pierre Vaccher [a], Julie Charton [b], Abdelhalim Guelzim [c], Daniel-Henry Caignard [d], Jean-Paul Bonte [a], Claude Vaccher [a,*]

[a] *Laboratoire de Chimie Analytique, EA 4034, Faculté des Sciences Pharmaceutiques et Biologiques, Université de Lille 2, 3 rue du Pr. Laguesse, BP 83, 59006 Lille Cédex, France*
[b] *INSERM U761 Biostructures and Early Drug Discovery, Université de Lille 2, Lille Pasteur Institute, 3 rue du Pr. Laguesse, BP 83, 59006 Lille Cédex, France*
[c] *Laboratoire de Dynamique et de Structure des Matériaux Moléculaires, UPRESA 8024, Université de Lille 1, Villeneuve d'Ascq Cédex, France*
[d] *Institut de Recherches Servier, 125 Chemin de Ronde, 78290 Croissy sur Seine, France*

Received 30 January 2007; received in revised form 16 January 2008; accepted 23 January 2008
Available online 12 February 2008

Abstract

The development of high performance liquid chromatography method on amylose-based stationary phases (Chiralpak AD) has permitted to achieve the preparative enantioseparation of one benzimidazole derivative, potent-AMP-kinase (AMPK) activator with satisfactory yields. Analytical enantioseparation method was optimized and validated to determine the enantiomeric purity. Using the UV detection, repeatability, limits of detection (LD) and quantification (LQ) were determined. Single-crystal X-ray analysis was successful to determine the absolute configuration of the individual enantiomers. A relation between the retention order and the absolute configuration of the enantiomers was established.

Keywords: AMPK; Enantiomeric separation; Chiral stationary phases; Chiralpak AD; Validation; X-ray crystallography

1. Introduction

The AMP-activated protein kinase (AMPK) is the central component of a protein kinase cascade that plays a major role in energy sensing. AMPK itself plays a key role in the regulation of metabolism within the muscle cell and has been already identified as a potential target for type 2 diabetes mellitus and obesity [1–4]. We recently described the synthesis and biological evaluation of benzimidazole derivative as potent AMPK activators [5].

Compounds were designed starting from the lead compound **1** (S27847, Fig. 1): firstly, by modification of the cyclohexylphenyl moiety and secondly, by introducing diversity on the aromatic moiety of the benzimidazole ring to obtain potential therapeutic agents. Many of them present high *in vitro* activation of the AMP-kinase on fresh rat hepatocytes. Those compounds present a chiral center and pharmacological studies of each enantiomer are so required. Chiral high performance liquid chromatography (HPLC) is one of the most rapid and efficient methods to obtain directly both enantiomers in high optical purity in a single step [6,7].

The aim of this study was to achieve preparative enantioselective HPLC separation of one of the most active racemic compounds to test the enantiomerically pure molecules so as to

* Corresponding author.
E-mail address: claude.vaccher@univ-lille2.fr (C. Vaccher).

0731-7085/$ – see front matter © 2008 Elsevier B.V. All rights reserved.
doi:10.1016/j.jpba.2008.01.048

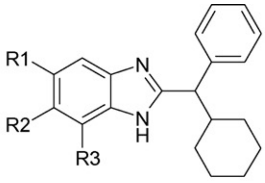

Compound	R1	R2	R3
1 (S27847)	H	H	H
2	CH_3	CH_3	H
3	H	Cl	H
4	H	CH_3	H
5	H	CH_3	CH_3
6	H	CF_3	H
7	H	F	H
8	OCH_3	OCH_3	H
9	H	OCH_3	H

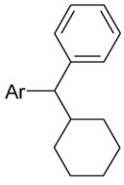

Compound	Ar
10	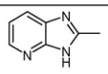
11	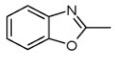
12	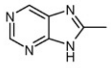
13	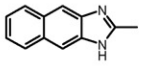
14	

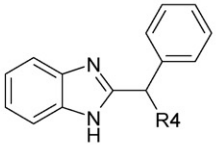

Compound	R4
15	CH_3
16	
17	

Fig. 1. Benzimidazoles derivatives.

enhance activity of benzimidazole derivatives. First, analytical methods were developed to determine the stationary and mobile phases which permitted the best enantiomeric separations: in literature benzimidazole derivatives chiral separations are mainly performed on Chiralpak AD as rabeprazole [8] or omeprazole [9–11]. Then, prior to the preparative scale, loading studies were performed to optimize the operational conditions. We then developed and validated analytical methods in order to quantify the enantiomeric purity. The absolute configuration of the individual enantiomers was established by X-ray analysis to obtain data for a mechanistic description of the chiral recognition in HPLC and of the ligand-receptor stereoselective interactions.

2. Experimental

2.1. Chiral liquid chromatography

Compounds **1**–**17** (Fig. 1) were prepared according to the synthetic pathway previously described [5], leading to a racemic mixture of enantiomers.

Analytical chiral chromatography was performed on a Chiralpak AD amylose column (tris-3,5-dimethylphenylcarbamate; 250 mm × 4.6 mm i.d.; 10 μm), a Chiralpak AS amylose column (tris-(*S*)-1-phenylethylcarbamate; 250 mm × 4.6 mm i.d.; 10 μm), a Chiralcel OD-H cellulose column (tris-3,5-dimethylphenylcarbamate; 250 mm × 4.6 mm i.d.; 5 μm) and on a Chiralcel OJ cellulose column (tris-4-methylbenzoate; 250 mm × 4.6 mm i.d.; 10 μm) (Daicel Chemical Industies, Baker, France). The ethanol, 1-propanol, 2-propanol and *n*-hexane were HPLC grade from Merck or Baker. All the solutions were filtered (0.45 μm), degassed with a Waters in-line degasser apparatus. Compounds were chromatographed by dissolving them in the alcohol of the corresponding mobile phase to a concentration of about 0.50 mM and passed through a 0.45 μm membrane filter prior to column loading. A constant mobile phase flow of 0.8 mL/min was provided by a gradient Waters 600E metering pump model equipped with a 7125 Rheodyne injector (20 μL loop). Detection was achieved with a Waters 996 photodiode array spectrophotometer at the maximum wavelengths (200 nm). Chromatographic data were collected and processed on a computer running with Empower software. Mobile phase elution was made isocratically using *n*-hexane and a modifier (ethanol, 1-propanol or 2-propanol) at various percentages. Chromatography was generally performed at 25 °C. The column void time (t_0) was considered to be equal to the peak of the solvent front and was taken from each particular run. It was about 4.07 min for Chiralpak AD (0.8 mL/min), and equal to the value obtained by injection of 1,3,5-tri-*tert*-butylbenzene used as a non-retained sample. Retention times were mean values of duplicate determinations.

For the semi-preparative scale, the same HPLC system was used with self-packed columns (Merck, 95 mm × 10 mm i.d.) loaded with bulk 20 μm stationary phases (AD) from Daicel (Daicel Chemical Industies, Baker, France). The temperature and mobile phase flow were, respectively, 25 °C and 1.5 mL/min and the sample loop was 20–100 μL.

The optical rotations of ethanol solutions (concentration of 3 mg/mL) using the Na D line (589 nm) were obtained using a Perkin-Elmer 241 polarimeter (Boston, MA, USA). The volume of the cell and the optical path were 1 mL and 10 cm, respectively. Measurements were performed at 26 °C.

The melting points were determined using a Büchi 530 capillary melting point apparatus.

2.2. X-ray crystal structure analysis

The (−)-**2** enantiomer was crystallized from a solution of ethanol. Crystal data: $C_{22}H_{26}N_2$, Mr = 318.45; colorless block; orthorhombic, space group $P2_12_12_1$ (no. 19), $a = 12.8937(7)$ Å, $b = 14.281(5)$ Å, $c = 20.003(7)$ Å, $V = 3683(2)$ Å^3, $Z = 8$, $D_c = 1.148$ Mg m^{-3}, $F(0\,0\,0) = 1376$, μ (Cu Kα) = 0.508 mm^{-1}, crystal dimensions 0.40 mm × 0.32 mm × 0.13 mm (Table 4).

Diffraction data were collected on an Enraf–Nonius Cad-4 diffractometer [12] using graphite monochromated Cu Kα radiation (λ = 1.5418 Å). Unit cell dimensions were determined by least-squares refinement of 25 reflections (θ range: 39.55–42.53°). Intensities were measured in the $\omega/2\theta$ scan mode ($\theta_{max} = 69.95°$). Data were reduced using the Wingx routine XCAD4 [13]. The intensities of five standard reflections were monitored every hour (decay 5.0% corrected). A total of 27620 reflections were collected according to the point group symmetry *mmm* resulting in 6968 unique reflections ($R_{int} = 0.042$ on F_0^2).

The structure of **2** was solved by direct methods using the program SIR92 [14]. Full matrix least-squares refinement (SHELXL-97) [15] was performed on F^2 for all unique reflections, minimizing $\sum w(F_0^2 - F_c^2)^2$, with anisotropic displacement parameters for the nonhydrogen atoms. The labelling of atoms is shown in Fig. 3a. The CH and CH_2 and CH_3 hydrogen atoms were included in idealized positions and refined with a riding model with C–H distances of 0.93 (Csp^2), 0.97 (CH_2) and 0.96 Å (CH_3) with U_{iso} constrained to 1.2 U_{eq} (CH and CH_2) and 1.5 U_{eq} (CH_3) of the parent atom except for the protons H(N), H(C11a), H(C11b), H(C10a) and H(C10b) (Fig. 3a): the position and the isotropic displacement parameters for these hydrogen atoms were refined freely.

The refinement (458 parameters, 6968 reflections) converged at $R_F = 0.0356$, $wR_{F^2} = 0.0894$ for 6103 reflections with $F_0 > 4\sigma(F_0)$ $w = 1/[\sigma^2(F_0^2) + (0.050P)^2 + 0.25P]$ where $P = (F_0^2 + 2F_c^2)/3$; $S = 1.05$. The absolute configuration was determined by refinement of the Flack parameter *x*-based on 3072 Bijvoet pairs. The reported configuration yielded $x = 0.04$ (7) [15,16].

3. Results and discussion

3.1. Chiral resolution

3.1.1. Analytical scale

The choice of optimal experimental conditions was achieved after screening of various parameters: type of the CSP, nature of the hexane–alcohol mobile phase (ethanol, 1-propanol or 2-propanol in the range 5–20% (v/v)). Since greater separation is preferred to permit greater sample loading in the preparative scale, the analytical conditions finally selected favor better resolutions to the detriment of retention times.

3.1.1.1. Column selectivity. Preliminary experiments were carried out on Chiralcel OD-H and OJ and Chiralpak AS. However, these trials could not result in any possible separation of the enantiomers of the different compounds. The Chiralpak AD show a broad applicability in resolving a great number of the studied racemic compounds.

3.1.1.2. Mobile phase selectivity. Concerning the mobile phase, it appears that best enantioseparations were obtained with ethanol; partial or total loss of resolution were generally observed using 2-propanol or 1-propanol for a same percentage of alcohol. In a same way the retention factors increase when changing from ethanol to 1-propanol and then to 2-propanol due to the relative lower polarity of the adduct. Whatever the molecule, it was observed when percentage of ethanol increases a decrease in retention factors, selectivities and resolutions.

Table 1
Conditions of the analytical enantioseparation on the Chiralpak AD for compounds **1–9** and chromatographic parameters: retention factor (k_1), enantioselectivity factor (α) and resolution (R_s)

Compound	Mobile phase	k_1	α	R_s
1	Hexane/ethanol: 80/20	0.28	1.22	<0.5[a]
	Hexane/ethanol: 90/10	0.71	1.43	1.16
	Hexane/ethanol: 95/5	2.95	1.39	1.48
	Hexane/2-propanol: 90/10	1.97	1.25	<0.5[a]
	Hexane/1-propanol: 90/10	0.97	1	n.r.
2	Hexane/ethanol: 80/20	0.26	2.40	2.15
	Hexane/ethanol: 90/10	0.93	2.34	3.89
	Hexane/ethanol: 95/5	3.56	2.22	5.26
	Hexane/2-propanol: 90/10	2.67	1.27	1.15
	Hexane/1-propanol: 90/10	1.09	1.43	1.70
3	Hexane/ethanol: 80/20	0.19	1	n.r.
	Hexane/ethanol: 90/10	0.66	1	n.r.
4	Hexane/ethanol: 80/20	0.34	1.23	<0.5[a]
	Hexane/ethanol: 90/10	1.21	1.25	0.99
5	Hexane/ethanol: 80/20	0.07	1	n.r.
	Hexane/ethanol: 90/10	0.30	1	n.r.
	Hexane/ethanol: 95/5	0.98	1	n.r.
	Hexane/2-propanol: 90/10	0.39	1	n.r.
	Hexane/1-propanol: 90/10	0.30	1.24	<0.5[a]
6	Hexane/ethanol: 80/20	0.07	1.23	<0.5[a]
	Hexane/ethanol: 90/10	0.28	1	n.r.
	Hexane/ethanol: 95/5	1.01	1.10	<0.5[a]
	Hexane/2-propanol: 90/10	0.62	1.38	<0.5[a]
	Hexane/1-propanol: 90/10	0.42	1	1
7	Hexane/ethanol: 80/20	0.17	1	n.r.
	Hexane/ethanol: 90/10	0.60	1.09	<0.5[a]
8	Hexane/ethanol: 80/20	0.67	1	n.r.
	Hexane/ethanol: 90/10	1.68	1.13	<0.5[a]
9	Hexane/ethanol: 80/20	0.35	1	n.r.
	Hexane/ethanol: 90/10	1.23	1.09	<0.5[a]
	Hexane/ethanol: 95/5	4.60	1.09	<0.5[a]
	Hexane/2-propanol: 90/10	2.32	1.63	2.14
	Hexane/1-propanol: 90/10	1.21	1.26	1.08

Concentration, 0.50 mM; flow rate, 0.8 mL/min; temperature, 25 °C.
[a] Shoulder; n.r.: no resolution.

3.1.1.3. Influence of the structure. This study was made with the hexane/ethanol 90/10 mobile phase.

We first studied the influence of the structural modifications of the phenyl moiety of the benzimidazole while maintaining the cyclohexylphenylmethyl group at the C2 position: compounds **1–9** (Table 1). When changing the nature of the R_2 substituent in **1** (H); **3** (Cl); **4** (CH_3); **6** (CF_3); **7** (F); **9** (OCH_3) the retention factors are 0.71, 0.66, 1.21, 0.28, 0.60, 1.23, respectively while only **1** (1.16) and **4** (0.99) are resolved. When changing the nature of two substituents R_1, R_2 in **1** (H, H); **2** (CH_3; CH_3); **8** (OCH_3; OCH_3) retention factors greatly increase (0.71; 0.93; 1.68) with R_s of 1.16; 3.89; <0.5. The resolution is very dependent of the position of the substituents as shown with compounds **2** (R_s: 3.89) and **5** (n.r.)

We secondly showed in the series **1** and **10–14** (Table 2) the influence of benzimidazolyl pattern by isosteric replacements. The change of a nitrogen *vs*. an oxygen (**1** and **11**) greatly increases the resolution (1.16–3.69) without changing the retention. The introduction of a supplementary aromatic (**1–13**) also enhances the resolution but with greater retention while the homologation (**1–14**) is no favorable to the separation. Introduction of one or two nitrogen atoms in the phenyl ring (**1–10** and **12**) does not lead to better results.

We then studied the influence of the nature of the substituent R_4 at the chiral center with the series **1** and **15–17** (Table 2). The retention factors are of same order but the resolution changes with 1.16; n.r.; 3.84; 2.92.

3.1.2. Semi-preparative scale

Preparative resolutions were run using column with enlarged diameter and enlarged granulometry (20 μm). During this semi-preparative step, experiments were performed to determine the effect of increasing sample load on the separation. The study of overloading was run with sample concentrations varying in the 0.5–30 mM range with a mobile phase flow of 1.5 mL/min. Although resolutions remain excellent, these overloadings are

Table 2
Conditions of the analytical enantioseparation on the Chiralpak AD for compounds **10**–**17** and chromatographic parameters: retention factor (k_1), enantioselectivity factor (α) and resolution (R_s)

Compound	Mobile phase	k_1	α	R_s
10	Hexane/ethanol: 80/20	0.29	1.33	<0.5[a]
	Hexane/ethanol: 90/10	0.58	1.36	1.03
11	Hexane/ethanol: 80/20	0.56	1.96	3.42
	Hexane/ethanol: 90/10	0.67	1.95	3.69
12	Hexane/ethanol: 80/20	0.44	1	n.r.
	Hexane/ethanol: 90/10	1.05	1.20	<0.5[a]
13	Hexane/ethanol: 80/20	0.46	1.97	2.54
	Hexane/ethanol: 90/10	1.57	1.91	3.87
14	Hexane/ethanol: 80/20	0.86	1	n.r.
	Hexane/ethanol: 90/10	2.15	1	n.r.
15	Hexane/ethanol: 80/20	0.28	1	n.r.
	Hexane/ethanol: 90/10	0.73	1.19	n.r.
16	Hexane/ethanol: 80/20	0.18	2.93	2.25
	Hexane/ethanol: 90/10	0.47	2.90	3.84
17	Hexane/ethanol: 80/20	0.29	1.98	1.73
	Hexane/ethanol: 90/10	0.83	1.97	2.92

Concentration, 0.50 mM; flow rate, 0.8 mL/min; temperature, 25 °C.
[a] Shoulder; n.r.: no resolution.

limited by the solubility of the compounds in the mobile phase. Then, the injected volumes (in the maximal concentration) were varied from 20 to 100 μL. They were limited by the touching band phenomenon. This up-scale study (30 mM and 100 μL) (Fig. 2) was run with 40 mg of compound **2** which is one of our

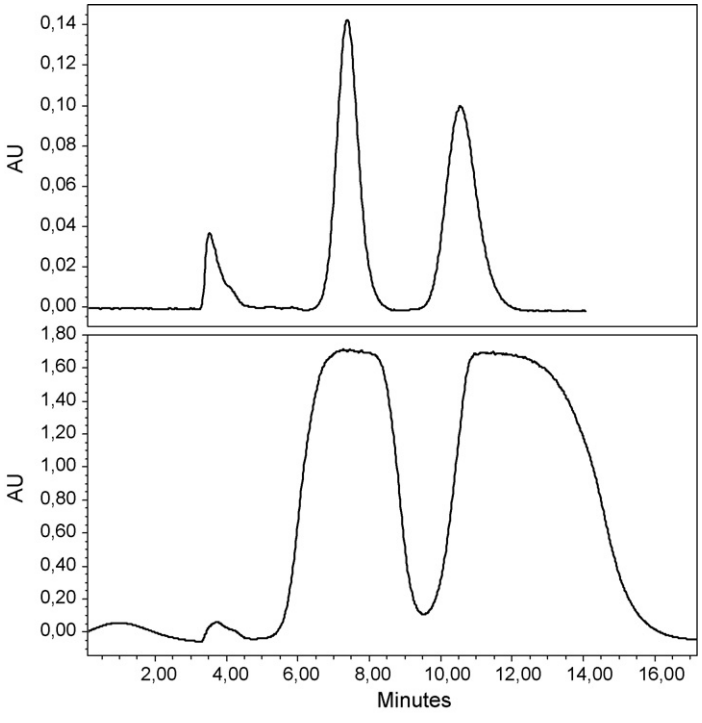

Fig. 2. Stacking chromatograms for the semi-preparative enantioseparation of **2** for various sample loading on Chiralpak AD; eluent, hexane–ethanol (90:10, v/v); temperature, 25 °C; flow rate, 1.5 mL/min); λ = 200 nm: (a) upper part: 0.5 mM and 20 μL injected and (b) lower part: 30 mM and 100 μL injected.

Table 3
Crystallographic data for (−)-(*R*)-(**2**)

Crystal data	(−)-(*R*)-**2**
Empirical formula	$C_{22}H_{26}N_2$
Crystal system	Orthorhombic
Space group	$P2_12_12_1$
a (Å)	12.8937(7)
b (Å)	14.281(5)
c (Å)	20.003(7)
V (Å^3)	3683 (2)
Z	8
d_{calc} (g cm^{-3})	1.148
μ (cm^{-1})	0.508
Refinement	
Refinement on	F^2
No. of refl. used in refinement	7411
R_1 ($I > 2\sigma(I)$)	0.0356
$wR_{2(all)}$	0.0894
S	1.04
No. of variables	458
Weighting scheme	$w = 1/[\sigma^2(F_0^2) + (0.050P)^2 + 0.25P]$ where $P = (F_0^2 + 2F_c^2)/3$
Absolute structure [4,5]	
$(\Delta/\sigma)_{max}$	0.062
$\Delta\rho_{min}$	−0.19 Å^{-3}
$\Delta\rho_{max}$	0.19 eÅ^{-3}

best AMPK activators [5]. The collected fractions from each isomers were pooled and evaporated under *vacuum* to give oily residues. They were crystallized in diisopropyl ether. The yields of the preparative separations are 71% and 65% for **2**(−) and **2**(+) for the first and second peaks, respectively.

3.2. Physico-chemical properties and determination of the absolute configuration

The specific rotations and the melting points are for **2**: $[\alpha]_D^{20} = -60.1$ and +59.8, T = 252–254 °C and 248–250 °C for the first and second peaks, respectively (the racemic melts at 214 °C).

A perspective drawing [17] of the molecular structure of **2**(−) with the crystallographic atomic labelling system is shown in Fig. 3a. The absolute stereochemistry at C10 has been established to be (*R*). The asymmetric unit of the crystal structure consists of two molecules (A and B) of **2** (Fig. 3b). For molecules A and B, the corresponding bond lengths and angles are almost the same. The two molecules A and B are interlinked by hydrogen bonds (Table 4). The most significant crystallographic data are summarized in Tables 3 and 4. The molecular conformation of **2** is shown in Fig. 3.

3.3. Determination of elution order

Enantiomer elution order is a very important topic in the determination of enantiomeric purity as well as the enantiorecognition mechanism. They were determined with various

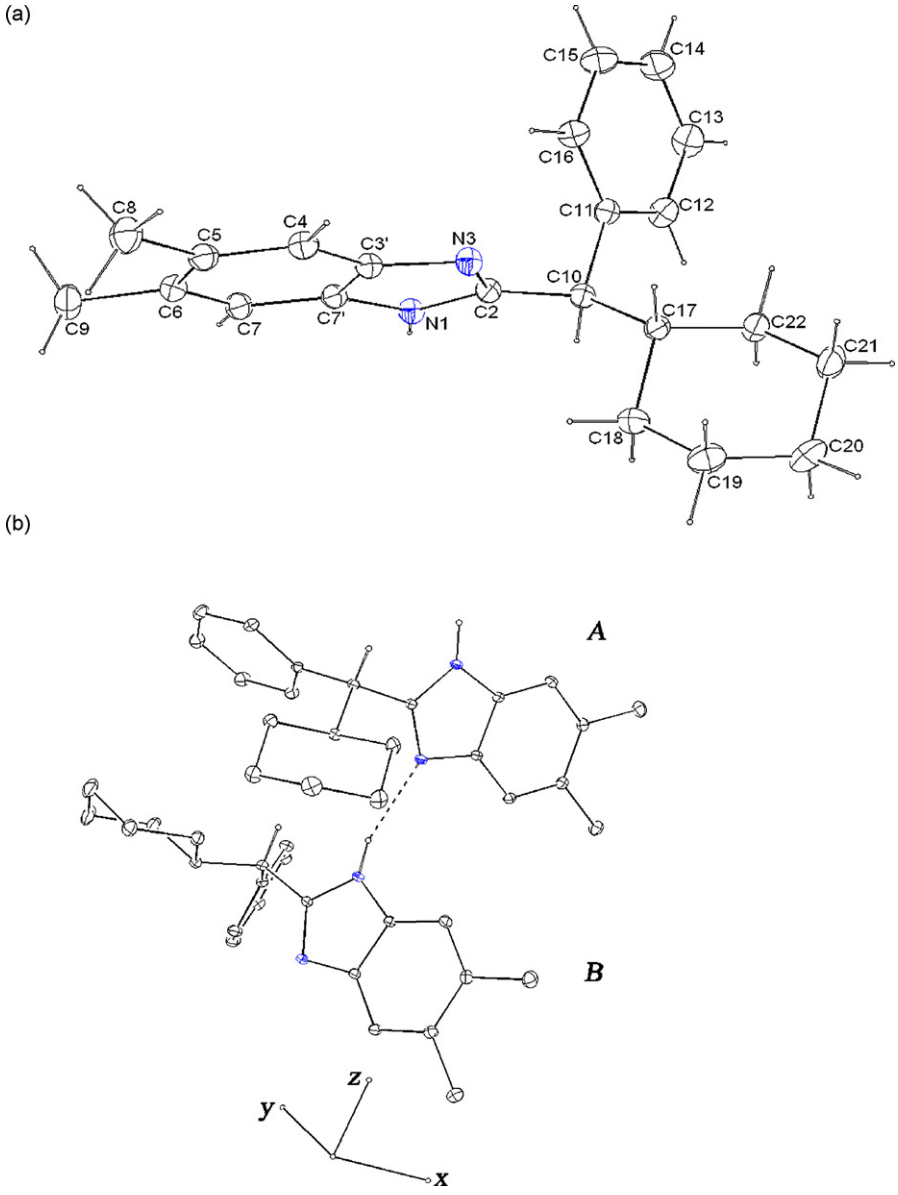

Fig. 3. Stereoscopic view and atomic numbering scheme of **2**(−)-(*R*).

mobile phases by injection of the pure enantiomers of **2**. It was observed that whatever the nature of the mobile phase (type and amount of the alcohol), order is the same. As all molecules exhibited similar three-dimensional structure and as the chiral recognition phenomenon is certainly the same, we could empirically suppose that the all first eluted peaks could be enantiomers of (*R*)-configuration and all second eluted peaks could be enantiomers of (*S*)-configuration.

3.4. Determination of the enantiomeric purities

The analytical method was validated. Standard solution (5.10^{-4} M) of racemate **2** was injected 10 times to evaluate the intra-day repeatability. Variation coefficients (CV%) were found to be less than 0.8% on retention times and less than 1.0% on peak areas for each enantiomer. The linear ranges were validated using five solutions covering the range from 4.10^{-4} to 6.10^{-4} M (80–120% of the target racemic concentration) and five solutions covering the range from 5.10^{-6} to 2.5×10^{-5} M (1–5%). Calibration curves were constructed from the compound peak areas and the corresponding concentrations. Triplicate injections of each sample were performed for each concentration. The correlation of the instrumental response (peak area) *vs*. compound concentration showed excellent linearity over the two ranges studied with $r^2 \geq 0.994$. Using ANOVA® software, it was proved that, according to the Student's *t*-test with the 95% confidence interval, both intercepts, for each racemate, are not significantly different from 0.

Comparison of slopes and intercepts of both calibration curves was also studied with ANOVA® software. It appears that slopes obtained in the two ranges are significantly different. Consequently, the determination of the enantiomeric purities must be evaluated with the concentrations of the majority and minority enantiomers, determined with the calibration curves in the

Table 4
Selected bond lengths (Å), angles (°), torsion angles (°), and hydrogen bond dimensions for (−)(*R*)-**2**

	Molecule A	Molecule B
Bond lengths		
N1–C2	1.360 (2)	1.360 (2)
N1–C7′	1.380 (2)	1.377 (2)
C2–N3	1.324 (2)	1.323 (2)
C2–C10	1.497 (2)	1.497 (2)
N3–C3′	1.394 (2)	1.400 (2)
C3′–C7′	1.394 (2)	1.391 (2)
C3′–C4	1.397 (2)	1.393 (2)
C4–C5	1.380 (2)	1.377 (2)
C5–C6	1.424 (2)	1.413 (2)
C5–C8	1.505 (2)	1.507 (2)
C6–C7	1.377 (2)	1.379 (2)
C6–C9	1.510 (2)	1.509 (3)
C7–C7′	1.391 (2)	1.390 (2)
C10–C11	1.526 (2)	1.516 (3)
C10–C17	1.547 (2)	1.547 (2)
Angles		
C2–N1–C7′	107.1 (1)	108.0 (1)
N3–C2–N1	112.6 (1)	111.8 (1)
N3–C2–C10	125.0 (1)	126.6 (1)
N1–C2–C10	122.3 (1)	121.5 (1)
C2–N3–C3′	105.0 (1)	105.3 (1)
N3–C3′–C7′	109.6 (1)	109.5 (1)
N3–C3′–C4	130.6 (1)	131.1 (1)
C7′–C3′–C4	119.8 (1)	119.4 (1)
C5–C4–C3′	119.6 (1)	119.5 (1)
C4–C5–C6	119.9 (1)	120.6 (2)
C4–C5–C8	119.7 (2)	119.3 (2)
C6–C5–C8	120.5 (2)	120.1 (2)
C7–C6–C5	120.6 (1)	120.3 (2)
C7–C6–C9	119.4 (2)	119.3 (2)
C5–C6–C9	120.0 (2)	120.4 (2)
C6–C7–C7′	118.7 (1)	118.4 (1)
N1–C7′–C7	133.0 (1)	132.8 (1)
N1–C7′–C3′	105.7 (1)	105.3 (1)
C7–C7′–C3′	121.4 (1)	121.9 (1)
Torsion angles		
C2–C10–C11	110.7 (1)	113.4 (1)
C2–C10–C17	110.3 (1)	112.3 (1)
C11–C10–C17	113.5 (1)	113.2 (1)
C10–C2–N3–C3′	178.4 (1)	−177.1 (2)
N3–C2–C10–C11	−87.2 (2)	−66.1 (2)
N1–C2–C10–C11	89.9 (2)	117.2 (2)
N3–C2–C10–C17	39.2 (2)	63.7 (2)
N1–C2–C10–C17	−143.6 (1)	−113.0 (2)
C2–C10–C11–C16	28.3 (2)	−109.9 (2)
C17–C10–C11–C16	−96.3 (2)	120.7 (2)
C2–C10–C11–C12	−152.6 (1)	73.9 (2)
C17–C10–C11–C12	82.8 (2)	−55.5 (2)
C2–C10–C17–C22	−175.0 (1)	178.7 (1)
C2–C10–C17–C18	61.4 (2)	55.6 (2)
C10–C17–C18–C19	−178.1 (2)	174.6 (2)

Hydrogen bond dimensions	D–H				
D–H. . .A	D–H (Å)	H. . .A (Å)	D–H–A (°)	D. . .A (Å)	Symmetry
N1A–H1A. . .N3B	0.948	1.925	177.90	2.872	[−*x* + 1/2, −*y* + 1, *z* + 1/2]
N1B–H1B. . .N3A	0.844	2.122	160.67	2.932	

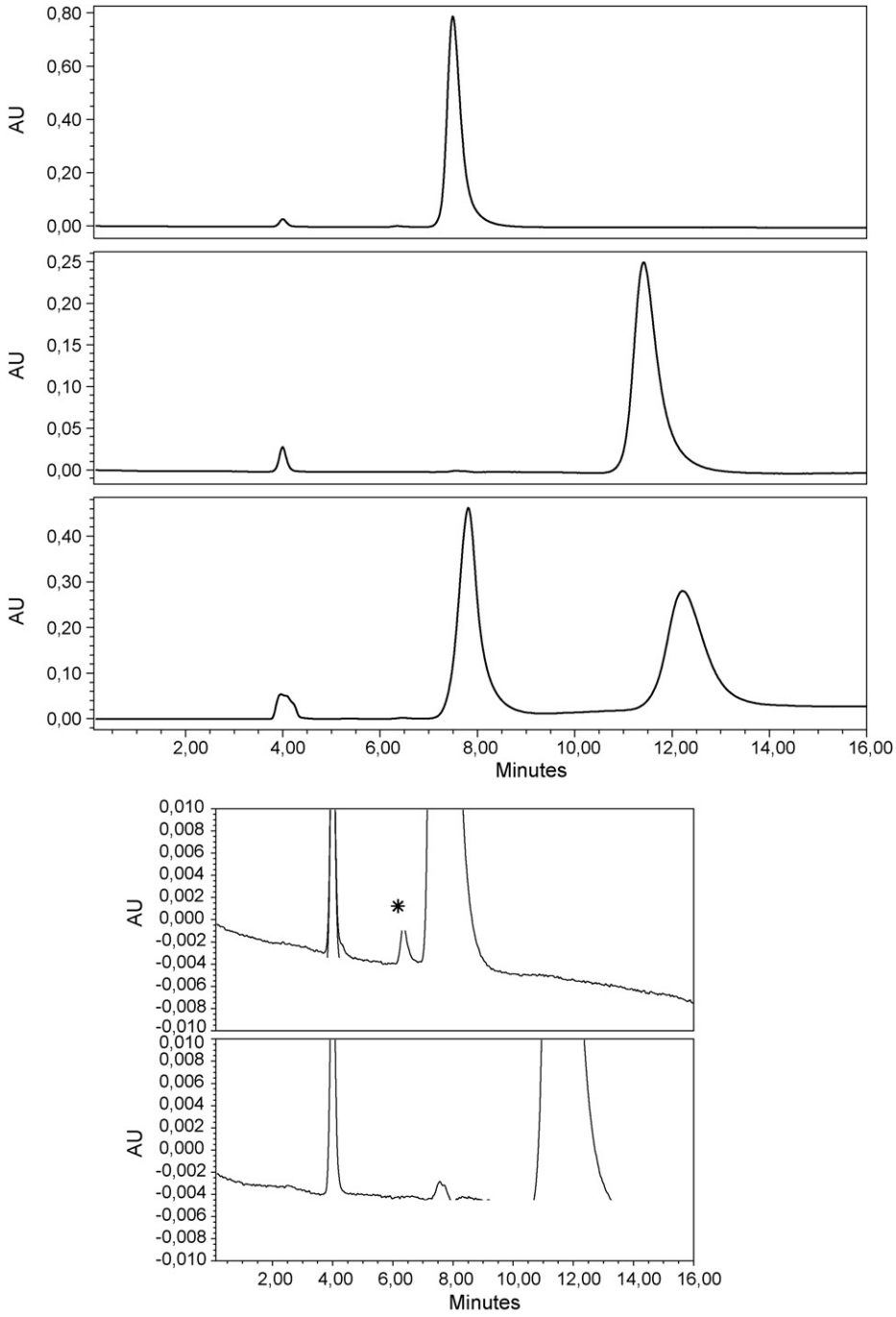

Fig. 4. Chromatograms of the **2** isolated enantiomers obtained on Chiralpak AD; eluent, hexane–ethanol (90:10, v/v); temperature, 25 °C; flow rate, 0.8 mL/min; λ = 200 nm; (*)impurity.

range 80–120% and 1–5%, respectively, and not with the area percentages directly. The limits of detection and quantification were determined with by serial dilutions in order to obtain signal/noise of 3 and 10 for LD and LQ, respectively. Since sharper peaks are obtained for the first eluted enantiomer, it presents lower limits of detection and quantification than the second eluted enantiomer. We obtained for LD and LQ 1.5 μg/L and 4.3 μg/L for compound **2**(−), which corresponds in our conditions to 0.1% and 0.3%, respectively. Fig. 4 presents the chromatograms obtained with each isolated isomer, which enantiomeric purity are for **2**(−) 99.81% and for **2**(+) 99.48%.

Preliminary chiral stability was undertaken: comparison of the enantiomeric purities, before and after the rotary evaporation (bath temperature 50 °C in the hexane/ethanol 90/10 mobile phase) revealed no significant racemization after 60 h.

In conclusion, analytical enantioseparations of seventeen benzimidazole derivatives, potent-AMP-activated protein kinase (AMPK) activators, was achieved by HPLC using amylose carbamate derivatives and optimized to obtain sufficient quantities of each enantiomer of one of them (**2**) for the evaluation of their pharmacodynamic and physico-chemical

properties (absolute configuration). Analytical methods have been developed and validated for each enantiomer to permit the quantification of their enantiomeric purity.

References

[1] W.W. Winder, D.G. Hardie, Am. J. Physiol. 277 (1999) E1–E10.
[2] D.E. Moller, Nature 414 (2001) 821–827.
[3] Y. Minokoshi, Y.B. Kim, O.D. Peroni, L.G. Fryer, C. Muller, D. Carling, B.B. Kahn, Nature 415 (2002) 339–343.
[4] N. Ruderman, M. Pentki, Nat. Rev. Drug Discov. 3 (2004) 340–351.
[5] J. Charton, S. Girault-Mizzi, M.A. Debreu-Fontaine, F. Foufelle, I. Hainault, J.G. Bizot-Espiard, D.H. Caignard, C. Sergheraert, Bio. Med. Chem. 14 (2006) 4490–4518.
[6] A. Shibukawa, T. Nakagawa, in: A.M. Krstulovic (Ed.), Chiral Separations by HPLC, Ellis Horwood, 1989.
[7] J. Dingenen, in: A Practical Approach to Chiral Separations by Liquid Chromatography, Subramanian G. (Eds.), New York 1994.
[8] R. Nageswara Rao, A. Narasu Raju, D. Nagaraju, Talanta 70 (2006) 805–810.
[9] Q.B. Cass, V.V. Lima, R.V. Oliveira, N.M. Cassiano, A.L.G. Degani, J. Pedrazzoli, J. Chromatogr. A 798 (2003) 275–281.
[10] R.M. Orlando, P.S. Bonato, J. Chromatogr. B 795 (2003) 227–235.
[11] H. Kanazawa, A. Ojada, M. Higaki, H. Yokota, F. Mashige, K. Nakahara, J. Pharm. Biomed. Anal. 30 (2003) 1817–1824.
[12] CAD-4 Software. V. 1.5c beta. Delft: Enraf–Nonius; 1994.
[13] K. Harms, S. Wocadlo, XCAD4—CAD4 Data Reduction, University of Marburg, Marburg, Germany, 1995.
[14] A. Altomare, G. Cascarano, C. Giacovazzo, A. Guagliardi, J. Appl. Crystallogr. 26 (1993) 343–350.
[15] G.M. Sheldrick, SHELXL-97: Program for the Refinement of Crystal Structures, University of Göttingen, Germany, 1997.
[16] H.D. Flack, Acta Crystallogr. A 39 (1983) 876–881.
[17] L.J. Farrugia, J. Appl. Crystallogr. 30 (1997) 565.